Nanoscale

COMMUNICATION

View Article Online
View Journal | View Issue

Cite this: *Nanoscale*, 2018, **10**, 1587

Received 11th December 2017,
Accepted 25th December 2017

DOI: 10.1039/c7nr09202d

rsc.li/nanoscale

Polydiacetylenic nanofibers as new siRNA vehicles for *in vitro* and *in vivo* delivery†

P. Neuberg,[a] I. Hamaidi,[b] S. Danilin,[b] M. Ripoll,[a] V. Lindner,[c] M. Nothisen,[a] A. Wagner,[d] A. Kichler,[a] T. Massfelder*[b] and J.-S. Remy*[a]

Polydiacetylenic nanofibers (PDA-Nfs) obtained by photopolymerization of surfactant 1 were optimized for intracellular delivery of small interfering RNAs (siRNAs). PDA-Nfs/siRNA complexes efficiently silenced the oncogene Lim-1 in the renal cancer cells 786-O *in vitro*. Intraperitoneal injection of PDA-Nfs/siLim1 downregulated Lim-1 in subcutaneous tumor xenografts obtained with 786-O cells in nude mice. Thus, PDA-Nfs represent an innovative system for *in vivo* delivery of siRNAs.

Since the discovery of RNA interference in 1998 by Andrew Z. Fire and Craig C. Mello, many attempts have been made to translate this strategy towards new approaches in the treatment of cancers in particular through specific silencing of deregulated oncogenes, responsible for cancer growth.[1,2] Nevertheless, despite enormous efforts in the design of carriers for siRNA, therapeutic success has been hampered by the low efficiency of siRNA delivery when used *in vivo*.

Here, we report on a new siRNA delivery system based on polydiacetylenic nanofibers, which have so far never been used for the intracellular delivery of biomolecules. Diacetylenic surfactants, based on a long C_{25} hydrocarbon chain containing conjugated triple bonds, are able to self-assemble into a large variety of supramolecular structures. The diacetylenic DA systems can be polymerized upon UV irradiation forming so-called PDA (PolyDiAcetylenic) systems initially discovered by G. Wegner in the early 1970s.[3–5] E. Doris's group pioneered on the exploration of the micellar forms of PDA, which are mostly monodisperse systems, for drug delivery.[6,7] Variations on the polar headgroups allowed for fine-tuning and optimization of their delivery properties. Indeed, cationic PDA-micelles promoted gene delivery while neutral oligo-ethylene decorated PDA-micelles favored hydrophobic drug formulation.[8,9] On the other hand, the introduction of pH sensitive imidazole groups (such as compound **2** in Fig. 1), allowed for efficient *in vitro* siRNA delivery.[10]

In initial formulation assays, we observed that diacetylenic surfactants **1** and **2** spontaneously reorganized in opaque gel-like structures upon prolonged storage at 5 °C under neutral or basic pH. This observation is in accordance with a similar gelation of PDA surfactants we described for propargylammonium PDA surfactants.[11] The diacetylenic surfactants **1** and **2** become extremely photosensitive in this gel like solutions, and they polymerize upon short irradiation times at 254 nm into deep blue aggregates. Photopolymerized PDA structures consisting in 2D monolayers (ribbons, in the blue form), twisted spirals or tubular structures are described in the literature, often in association with chiral headgroups, such as small peptides and modified amino acids.[12–15]

The polymeric aggregates formed by photopolymerization of **1** or **2** dissolve under acidic conditions to form small red nanofibers, which are highly fluorescent. The red transparent solutions of polymerized histidine surfactant **2** are composed of extended fibers, ranging from 10 to 50 μm in length. They are highly resistant to shearing forces. They could not be

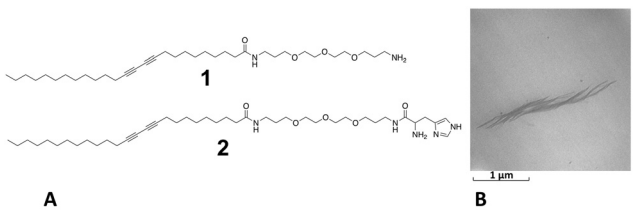

Fig. 1 (A) Structure of diacetylenic surfactant **1** and histidine analogue **2**. (B) Low voltage electron microscopy of PDA-Nfs obtained from **1** after photopolymerization and sonication (red fluorescent form).

[a]*V-SAT Laboratory, Vectors: Synthesis and Therapeutic Applications, Labex Medalis, CAMB UMR7199 CNRS-Université de Strasbourg, Faculty of Pharmacy, Illkirch, France. E-mail: remy@unistra.fr*
[b]*Laboratory "Voies de signalisation du développement et du stress cellulaire dans les cancers digestifs et urologiques" (VSDS), Team 3 "Signalisation et communication cellulaires dans les cancers du rein et de la prostate" - UMR_S 1113, INSERM-Université de Strasbourg, France. E-mail: massfeld@unistra.fr*
[c]*Hôpitaux universitaires de Strasbourg, Hôpital de Strasbourg-Hautepierre, Department of Pathology, Strasbourg, France*
[d]*Laboratory of Bio-FunctionalChemistry (BFC), Labex Medalis, CAMB UMR7199 CNRS-Université de Strasbourg, Faculty of Pharmacy, Illkirch, France*

†Electronic supplementary information (ESI) available: Details of chemical synthesis, preparation of PDA-Nfs and biophysical characterization, detailed *in vitro* and *in vivo* results. See DOI: 10.1039/c7nr09202d

further fragmented even under harsh conditions (such as sonication or heating) to obtain smaller sized fibers, such as would be required for cell delivery assays. Optimization of the formulations with a diverse set of diacetylenic surfactants allowed us to select surfactant **1** as the best candidate for intracellular delivery as it could form consistently smaller fibers, termed here **PDA-Nfs** (micrographs of the fibers obtained from **1** and **2** are shown in ESI-1A and B†). The PDA-Nfs formed with surfactant **1** were then explored in *in vitro* and *in vivo* siRNA transfection experiments.

The selected diacetylenic monomer (**1**) has been synthetized by coupling 4,7,10-trioxa-1,13-tridecanediamine on the NHS ester of commercial 10,12-pentacosadiynoic acid (see ESI for detailed synthesis procedure, and Fig. S2 and S3† for the NMR and mass spectra of compound **1**).

The optimized formulations were obtained by injecting hot concentrated solutions of **1** into 30% ethanol/water at 5 °C. The obtained gel-like solutions were polymerized under hard UV-light at 254 nm in a UV-Crosslinker, where they converted into red PDA-Nfs (see ESI for detailed procedure and Fig. S4 and S5†). Such color change are supposed to originate from distortion of π-conjugated backbone of PDA, due to a transition from 2D monolayer, sheet like structures into tubular twisted forms.[16] Some PDA-liposome biosensors rely on these chromatic properties, where a physical or chemical stimulus induces this blue-red color change.[17,18] Some are used for diagnosis of prostate cancer.[19]

We further characterized these PDA-Nfs of **1** by physicochemical methods, such as UV-Vis and fluorescence spectroscopy, dynamic light scattering and low voltage electron microscopy (see ESI† for detailed biophysical characterization, Fig. 1B, 2A, S4 and S5†).

The fluorescence absorption and excitation spectra are shown in Fig. 2A. Interestingly the maximum excitation wavelength is separated by a wide bandwidth between 550 and 646 nm (Stokes shift of about 100 nm).

The hydrodynamic diameter of the PDA-nanofibers was measured by dynamic light scattering experiments. Their mean size by intensity is 780 nm. The same fiber solution diluted 10-fold showed a zeta potential of +52 mV, confirming the presence of positively charged amine functions at the outer side of the nanofibers (see Fig. S6†).

Complexation of anionic siRNA molecules in neutral buffer conditions, and analysis by gel electrophoresis show that siRNA is complexed at low N/P values around 4. This N/P ratio is defined as the total amine content of the PDA-Nfs *versus* the number of phosphate groups present in the siRNA (see Fig. S7A†). Interestingly, similar complexation has been achieved with extensively dialyzed nanofibers, where all residual monomer has been removed, confirming indirectly the high polymerization efficiency under the conditions of nanofiber preparation (see ESI for dialysis purification and complexation assays, in Fig. S7B†).

Up to 80% silencing could be obtained with 10 nM siLuc (siRNA targeting the luciferase reporter gene; at N/P values from 12 to 20; see Fig. 3). Total protein quantification of transfected cells, compared to untreated ones, shows low toxicity of the PDA-Nfs formulated siRNAs.

The PDA-Nfs/siRNA complexes also maintained high silencing efficiency in 10% serum conditions (see Fig. S8†), and they compared favorably to commercial transfection reagent INTERFERin (from POLYPLUS-transfection).

In order to prove the efficiency of the PDA-Nfs/siRNA complexes on another cell line, the 786-O human renal cancer cells was selected. 786-O cell line represents one of the most used model to study Clear Cell renal Cell carcinoma (CCC). CCC is the most common and aggressive form of kidney cancer in adult (>75% of kidney cancer cases), and remains resistant to current anticancer therapies.

Luciferase expressing 786-O-Luc cell line was used for the optimization of the delivery conditions of siRNA with the PDA-Nfs/siRNA. As with the A549-Luc cells, a highly efficient silencing of the luciferase reporter gene was observed in 786-O-Luc cells, as indicated by direct bioluminescence

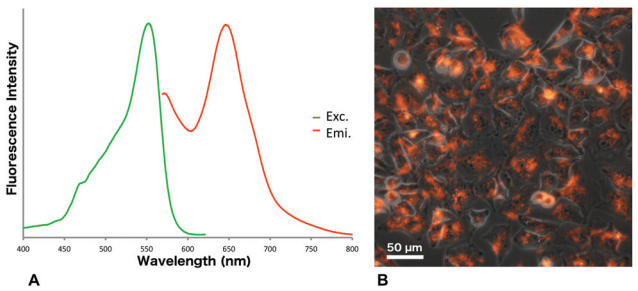

Fig. 2 (A) Fluorescence excitation (green) and emission (orange) spectra of PDA-Nfs (**1**). (B) Fluorescence microscopy of A549-Luc cells transfected with PDA-Nfs/siRNA showing an overlay of phase contrast picture and fluorescence image. A strong internalization of PDA-Nfs/siRNA complexes (with a N/P = 13 and a final siRNA concentration of 10 nM) is observed after 24 hours by fluorescence microscopy using the intrinsic fluorescence of the PDA-Nfs.

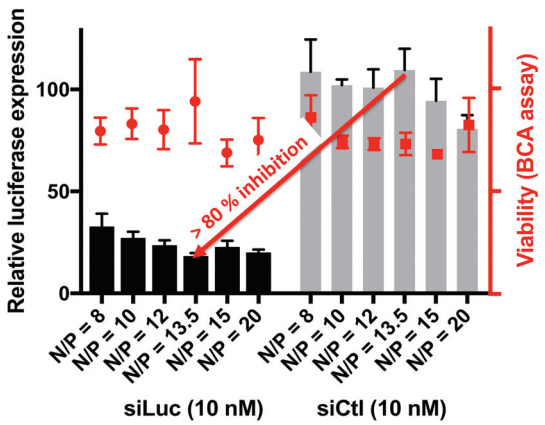

Fig. 3 siLuc delivery in A549-Luc cell line at 10 nM siRNA concentration and various N/P ratios (optimal N/P for this cell line at N/P 13.5 shows a silencing of 82%). Viability is measured by total protein quantification and compared to untreated cells.

imaging of the cell culture plates. In this cell line the optimal N/P values ranged between N/P 5 and 10 (see ESI for bioluminescence assay and cell density measurements, Fig. S9†).

Dr. Massfelder's group has recently identified the developmental transcription factor Lim-1 as an oncogene in CCC regulating tumor growth.[20,21] The selected 786-O cell line expresses constitutively the Lim-1 oncogene.[20]

We evaluated the capacity of PDA-Nfs to silence endogenous Lim-1 in 786-O. As shown in Fig. 4, the PDA-Nf/siLim allowed to inhibit the expression of Lim-1 by more than 80% at the various PDA-Nfs concentrations tested. The relative expression of Lim-1 has been measured by qPCR analysis in comparison to cyclophilin used as a reference gene (48 hours of treatment at 10 nM siLim1 concentration; Fig. 4). The RNA interference efficiency has been calculated by comparing the level of Lim-1 expression on PDA-Nfs/siLim1 treated cells to that of PDA-Nfs/siCtl. As a positive control for siRNA transfection we used jetPrime reagent (from POLYPLUS-transfection).

In order to evaluate the capacity of the PDA-Nfs to silence a gene that is even highly expressed, we used a stable 786-O clone overexpressing Lim-1 by up to 80 times. This clone was treated with 10 nM of siLim1 and siCtl complexed with 4 μM amine concentration of PDA-Nfs (N/P = 10). RT-qPCR analysis shows a decrease of Lim-1 expression by approx. 90% (see Fig. S10†).

Finally, we tested the efficacy of nanofibers to carry small interfering RNA *in vivo*. Nude mice bearing subcutaneous human 786-O tumors were treated by a single intraperitoneal injection of PDA-Nf/siLim (n = 6), PDA-Nfs/siCtl (n = 5) complexes or untreated (n = 4). Forty eight hours after treatment, animals were euthanized and the tumors were harvested. Each tumor was cut in 2 parts, one for Western blot analysis, and the other part for RT-qPCR analysis. RT-qPCR analysis showed a significant decrease of Lim-1 expression in PDA-Nfs/siLim1 group, as compared to PDA-Nfs/siCtl (see Fig. 5A; and ESI† for statistical analysis). These results were confirmed by Western blot analysis on the pooled samples. We clearly observed a decrease of Lim-1 expression in PDA-Nfs/siLim group as compared to PDA-Nfs/siCtl or untreated groups (Fig. 5B, experimental details in ESI†).

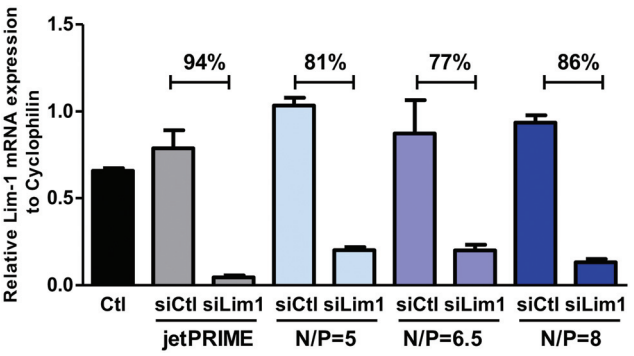

Fig. 4 Reduced expression level of endogenous Lim-1 gene in 786-O cells after 48 h treatment with specific (siLim1) and control siRNA at 10 nM siRNA concentration and various concentrations of PDA-Nfs (N/P = 5 to N/P = 8). JetPRIME reagent (POLYPLUS-transfection) was used as a positive control for siRNA delivery.

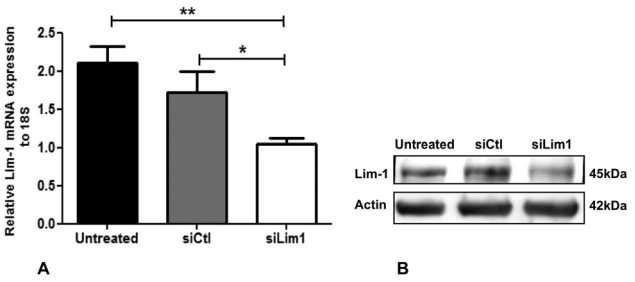

Fig. 5 *In vivo* silencing efficiency of siRNA targeting Lim-1 oncogene (siLim1) in subcutaneous xenografted 786-O cells in nude mice. (A) qPCR quantification of the expression level of Lim-1 gene relative to the housekeeping gene 18S. Average results shown as mean ± s.e.m., Untreated n = 4, PDA-Nfs/siCtl n = 5, PDA-Nfs/siLim1 n = 6; $^{**}P < 0.01$ from Ctl; $^{*}P < 0.05$ from siCtl (B) Western blot analysis of the expression level of the Lim-1 gene as compared to the actin protein. Each plot represents a pool of all tumor extracts from the same group.

The siRNA/PDA-Nfs complexes used in these *in vivo* experiments were also characterized by DLS and zeta potential measurement. At the chosen N/P = 6 ratio the PDA-Nfs concentration is sufficient to maintain positive zeta potential values >35 mV of the siRNA complexes, ensuring that the complexes do not tend to aggregate (see ESI for detailed analysis, and Fig. S11†).

Biodistribution of i.p. injected PDA-Nf/siRNAs was assessed by histological analysis of sections from paraffin embedded organs of mice euthanized at 1 hour or at 48 hours after administration of PDA-Nfs. At 1 h they were detected in blood samples, as well as in various organs, such as the spleen (high abundance), liver, lung and kidney by fluorescence microscopy (see ESI for detailed experimental procedure and Fig. S12†). However the fluorescence of the PDA-Nfs could not be detected any more, neither in the organs from mice taken at 48 h, nor in their blood samples. At this time point the PDA-Nfs seemed metabolized or cleared from the body. This observation is in accordance with a supposed progressive clearance by the kidneys, as urine samples taken from mice taken at 48 h but not at 1 h showed weak presence of PDA-Nfs. Furthermore the fluorescent PDA-Nfs could also be detected in tumor samples from mice sacrificed at 48 hours after i.p. administration, where we have shown that they lead to specific silencing of the Lim-1 oncogene (see ESI for detailed microscopic analysis of the histological sections, and Fig. S13†). In all these experiments mice had normal behavior and no signs of inflammation nor discomfort were observed after injections. This clearly shows that these new siRNA formulations are safe. We note that some larger particles such as cationic tyrosine modified PEI-siRNA complexes are able to diffuse to tumor xenografts after intraperitoneal injection.[22] On the other hand elongated multiwalled carbon nanotubes of μm length have been described to be able to diffuse in the living organism reaching various organs dependent on the shape and nature of the nanotubes.[23] All animal procedures were performed in accordance with the Guidelines for Care and Use of Laboratory Animals of

Animal Care Facility at the Faculty of Medicine at the University of Strasbourg (France) and were approved by the Animal Ethics Committee of CREMAS (Comité régional d'éthique en matière d'expérimentation animale de Strasbourg).

Conclusion

In the present work, we were able to show for the first time that PDA-Nfs can be promising delivery agents for siRNAs. Surfactant (**1**) allows for the generation of relatively small nanofibers that are able to internalize efficiently into cells. The PDA nanofibers associated with a siRNA targeting a reporter gene (luciferase gene in A549-Luc and 786-O-Luc cell lines) lead to a very efficient silencing.

In vitro, the PDA-Nfs/siLim1 efficiently silenced by more than 80% the expression of the Lim-1 oncogene in the 786-O human CCC cell line. Furthermore, when administered intraperitoneally, the PDA-Nfs were able to deliver siRNA into subcutaneously grown tumors, where they led to specific silencing of the targeted Lim-1 oncogene. By analyzing the biodistribution of the PDA-Nfs, we proved that these nanofiber systems diffuse in the bloodstream and reach various organs as well as the targeted tumors. They were cleared from the body 48 hours post-injection presumably by renal excretion, as the PDS-Nfs could then be detected in urine samples.

Taken together, we found that PDA-Nfs are a promising and highly efficient new class of self-organized siRNA vectors for *in vitro* and *in vivo* applications, with good biodistribution profiles in the body.

Conflicts of interest

There are no conflicts to declare.

Acknowledgements

This PDA-Nanofiber system has been patented in 2016 under: EP16305367. We thank the Labex Medalis and FRM Foundation (Fondation pour la Recherche Médicale, Chimie pour la Médicine) for post-doctoral grants for PN and SD. MR and IH received financial doctoral support from the University of Strasbourg. We thank Dr F. Daubeuf from TechMed'Ill for biodistribution study.

Notes and references

1 M. E. Davis, *Mol. Pharm.*, 2009, **6**, 659–668.
2 K. A. Howard, *Adv. Drug Delivery Rev.*, 2009, **61**, 710–720.
3 G. Wegner, *Z. Naturforsch., B*, 1969, **24**, 824–832.
4 G. Wegner, *Makromol. Chem.*, 1972, **154**, 35–48.
5 B. Tieke, G. Wegner, D. Naegele and H. Ringsdorf, *Angew. Chem., Int. Ed. Engl.*, 1976, **15**, 764–765.
6 N. Mackiewicz, E. Gravel, A. Garofalakis, J. Ogier, J. John, D. M. Dupont, K. Gombert, B. Tavitian, E. Doris and F. Ducongé, *Small*, 2011, **7**, 2786–2792.
7 E. Gravel, B. Thézé, I. Jacques, P. Anilkumar, K. Gombert, F. Ducongé and E. Doris, *Nanoscale*, 2013, **5**, 1955–1960.
8 E. Morin, M. Nothisen, A. Wagner and J.-S. Remy, *Bioconjugate Chem.*, 2011, **22**, 1916–1923.
9 P. Neuberg, A. Perino, E. Morin-Picardat, N. Anton, Z. Darwich, D. Weltin, Y. Mely, A. S. Klymchenko, J.-S. Remy and A. Wagner, *Chem. Commun.*, 2015, **51**, 11595–11598.
10 M. Ripoll, P. Neuberg, A. Kichler, N. Tounsi, A. Wagner and J.-S. Remy, *ACS Appl. Mater. Interfaces*, 2016, **8**, 30665–30670.
11 E. Morin, J.-M. Guenet, D. D. Díaz, J.-S. Remy and A. Wagner, *J. Phys. Chem. B*, 2010, **114**, 12495–12500.
12 L. Hsu, G. L. Cvetanovich and S. I. Stupp, *J. Am. Chem. Soc.*, 2008, **130**, 3892–3899.
13 M. van den Heuvel, D. W. P. M. Löwik and J. C. M. van Hest, *Biomacromolecules*, 2010, **11**, 1676–1683.
14 B. E. I. Ramakers, M. van den Heuvel, N. Tsichlis i Spithas, R. P. Brinkhuis, J. C. M. van Hest and D. W. P. M. Löwik, *Langmuir*, 2012, **28**, 2049–2055.
15 E. Gravel, J. Ogier, T. Arnauld, N. Mackiewicz, F. Ducongé and E. Doris, *Chem. – Eur. J.*, 2012, **18**, 400–408.
16 S. R. Diegelmann, N. Hartman, N. Markovic and J. D. Tovar, *J. Am. Chem. Soc.*, 2012, **134**, 2028–2031.
17 B. Yoon, S. Lee and J.-M. Kim, *Chem. Soc. Rev.*, 2009, **38**, 1958–1968.
18 D. H. Kang, H.-S. Jung, J. Lee, S. Seo, J. Kim, K. Kim and K.-Y. Suh, *Langmuir*, 2012, **28**, 7551–7556.
19 I. K. Kwon, J. P. Kim and S. J. Sim, *Biosens. Bioelectron.*, 2010, **26**, 1548–1553.
20 V. Dormoy, C. Béraud, V. Lindner, L. Thomas, C. Coquard, M. Barthelmebs, D. Jacqmin, H. Lang and T. Massfelder, *Oncogene*, 2011, **30**, 1753–1763.
21 V. Dormoy, D. Jacqmin, H. Lang and T. Massfelder, *Anticancer Res.*, 2012, **32**, 3609–3617.
22 A. Ewe, S. Przybylski, J. Burkhardt, A. Janke, D. Appelhans and A. Aigner, *J. Controlled Release*, 2016, **230**, 13–25.
23 J. T.-W. Wang, C. Fabbro, E. Venturelli, C. Ménard-Moyon, O. Chaloin, T. Da Ros, L. Methven, A. Nunes, J. K. Sosabowski, S. J. Mather, M. K. Robinson, J. Amadou, M. Prato, A. Bianco, K. Kostarelos and K. T. Al-Jamal, *Biomaterials*, 2014, **35**, 9517–9528.

